Remaining Useful Life Estimation of Lithium-Ion Batteries based on Thermal Dynamics

Dong Zhang, Satadru Dey, Hector E. Perez, Scott J. Moura

Abstract— **Longevity remains one of the key issues for Lithium-ion (Li-ion) battery technology. On-board Intelligent Battery Management Systems (BMS) implement health-conscious control algorithms in order to increase battery lifetime while maintaining the performance. For such algorithms, the information on Remaining Useful Life (RUL) of the battery is crucial for optimizing the battery performance and ensuring minimal degradation. However, accurate prediction of RUL remains one of the most challenging tasks until this date. In this paper, we present an online RUL estimation scheme for Li-ion batteries, which is designed from a thermal perspective. The key novelty lies in (i) leveraging thermal dynamics to predict RUL and, (ii) developing a hierarchical estimation algorithm with provable convergence properties. The algorithm consists of three stages working in cascade. The first two stages estimate the core temperature, State-of-Charge (SOC) and battery capacity based on a combination of thermal and Coulombic SOC model. The third stage receives this capacity information and in turn identifies a capacity fade aging model. Finally, we estimate the RUL by predicting the battery capacity fade over the cycles utilizing the identified aging model. A combination of sliding mode observers and nonlinear least-squares algorithm is utilized for designing the estimators. Simulation results illustrate the performance of the proposed RUL estimation scheme.**

I. Introduction

With the rapid evolution of smart grid technologies and electrified vehicles, the Lithium-ion (Li-ion) battery has become a prominent device for energy storage. Over the last decade, interest in this topic has dramatically increased and a substantial body of research has emerged on improving battery performance and safety. Essentially, an intelligent BMS implements real-time control/estimation algorithms that enhance battery performance while improving safety. One of the crucial functions of such BMS is to estimate the Remaining Useful Life (RUL) [1]. Accurate RUL estimation is still an unsolved problem in BMS research.

The existing literature contains several approaches to RUL estimation. Broadly, these approaches can be categorized into offline and online approaches. Offline approaches generally develop RUL models in specific laboratory settings with access to large amounts of battery data under varying operating conditions. Liu *et al*. developed a data-driven adaptive recurrent neural network (ARNN) trained using history resistance data at two different temperatures for battery RUL prediction [2]. A model based offline RUL prediction using relevance vector machines (RVMs) and particle filters (PFs) were examined in [3]. Tang *et al*. proposed a RUL prediction method based on the Wiener process with measurement error and offline parameter estimation [4]. Although these offline approaches significantly contribute towards this research area, their applicability for real-time purpose is limited due to the following reasons: (i) in real-time, we have access to very limited amounts of data; (ii) in practice, battery degradation depends significantly on the usage patterns. Therefore, a single offline RUL scheme may not be sufficient for these cases. These facts motivate the necessity of online approaches for RUL estimation.

The online RUL estimation approaches operate on real-time BMS processors utilizing real-time measurements. Generally, online approaches are comparatively more challenging than their offline counterparts due to lack of measured information and limited computation power. A few studies have investigated this. Zhou *et al*. used mean voltage falloff (MVF) as a health indicator to quantify the capacity degradation, thanks to high correlation between MVF and capacity [5]. Orchard *et al*. developed a risk-sensitive particle filtering based approach for accurate RUL and end-of-life (EOL) estimation in [6]. Data-driven capacity estimation approaches, such as artificial neural network (ANN) and Relevance Vector Machine (RVM), were examined in [7], [8]. However, none of the aforementioned approaches explore RUL estimation from a thermal perspective. In light of these existing approaches, the main contributions of the paper are the following: (i) we exploit electro-thermal coupling to predict RUL of the battery in terms of capacity fade; (ii) from a theoretical perspective, we develop a hierarchical estimation algorithm with mathematically provable convergence and robustness properties.

The proposed online RUL estimation scheme is composed of a hierarchical structure with three stages. In Stage 1, core temperature and heat generation are estimated based on a two-state thermal model. Stage 2 estimates SOC and capacity using the coupling between thermal and electrical dynamics. Finally, Stage 3 uses estimated capacity and core temperature, as well as input current to identify a capacity fade model. A combination of sliding mode observers [9] and least-squares algorithm is used for the estimator design, where the convergence of each estimation process is carefully examined. The choice of sliding mode observer is due to its provable finite time convergence and robustness properties. This identified aging model further predicts the battery EOL, defined as a 20% decrease of the original cell capacity [10].

The paper is organized as follows: Section II presents battery electrical, thermal, and aging models. Section III

Dong Zhang, Satadru Dey, Hector E. Perez, Scott J. Moura are with Energy, Controls, and Applications Lab (eCAL) in Civil and Environmental Engineering, University of California, Berkeley, CA 94720, USA (e-mail: {dongzhr, satadru86, heperez, smoura}@berkeley.edu)

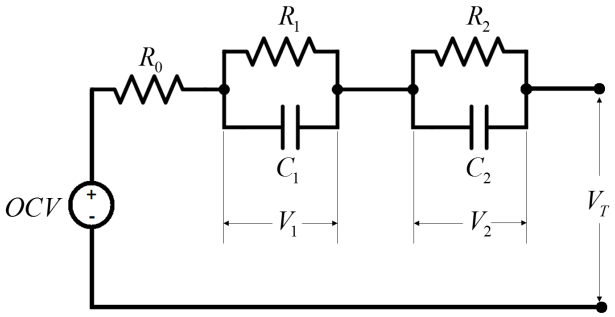

Fig. 1: Schematic of Equivalent Circuit Model

discusses sliding mode observers with stability analyses, and least-squares algorithm for parameter identification. Section IV discusses the simulation results for a particular charge-discharge cycle. Conclusions are drawn in Section V.

II. Battery Model

This paper utilizes an equivalent circuit model (ECM) that captures the electrical dynamics, and a two-state thermal model that captures battery surface and core temperature dynamics [11]. We also consider a cycle-life battery aging model from [12]. In the following subsections, we describe these models in detail.

A. Electrical Model

Consider the ECM presented in Figure 1, which idealizes a battery as an open-circuit voltage (OCV) in series with two resistor-capacitor (R-C) pairs, and an internal resistor (R_0). The state space dynamics and output are given by:

$$\frac{dSOC(t)}{dt} = -\frac{I(t)}{C_{bat}} \tag{1}$$

$$\frac{dV_1(t)}{dt} = -\frac{1}{R_1C_1}V_1(t) + \frac{1}{C_1}I(t) \tag{2}$$

$$\frac{dV_2(t)}{dt} = -\frac{1}{R_2C_2}V_2(t) + \frac{1}{C_2}I(t) \tag{3}$$

$$V_T(t) = OCV(SOC) - V_1(t) - V_2(t) - I(t)R_0 \tag{4}$$

where $I(t)$ is the input current, and we specify positive for discharge and negative for charge. C_{bat} is the battery charge capacity in Ampere-second, and V_T denotes terminal voltage.

B. Thermal Model

A two-state lumped thermal model of a cylindrical battery is adopted from [11]. The model states are core temperature (T_c) and surface temperature (T_s):

$$C_c\frac{dT_c(t)}{dt} = \frac{T_s(t) - T_c(t)}{R_c} + \dot{Q}(t) \tag{5}$$

$$C_s\frac{dT_s(t)}{dt} = \frac{T_f(t) - T_s(t)}{R_u} - \frac{T_s(t) - T_c(t)}{R_c} \tag{6}$$

$$\dot{Q}(t) = I(t)\Big(OCV(SOC) - V_T(t) - T(t)\frac{dU}{dT}\Big) \tag{7}$$

where R_c, R_u, C_c and C_s represent heat conduction resistance, convection resistance, core heat capacity, and surface heat capacity, respectively. $\dot{Q}(t)$ is internal heat generation. Heat generation from resistive dissipation and entropic heat are considered, where U is the equilibrium potential and $T(t)$ is the average of surface and core temperature. Following [11], we assume the coolant flow rate is constant and the ambient temperature T_f is nearly constant. The thermal parameters used in this work have been identified and validated on a $LiFePO_4$/LiC_6 A123 26650 cell [11].

C. Aging Model

A cycle-life aging model is adopted from [12]. Experimental data strongly suggests that time (Ah-throughput), temperature and C-rate significantly affect capacity fade. They propose an empirical capacity fade model, given as:

$$P_{loss} = B(c)\cdot\exp\left(\frac{E_a(c)}{RT_c}\right)(Ah)^z \tag{8}$$

where P_{loss} is the capacity loss percentage, c is C-rate, $B(c)$ is the pre-exponential factor, and R is the universal gas constant. Ah is ampere-hour throughput. Moreover, $E_a(c)$ and z are the activation energy and power law factor, respectively. A cycle-life capacity model can be derived accordingly:

$$\begin{aligned} C_{bat}(N) &= \Big(1 - \frac{P_{loss}}{100}\Big)C_{bat}(0) \\ &= \Big[1 - a\cdot\exp\Big(\frac{b}{RT_c}\Big)(Ah)^z\Big]C_{bat}(0) \end{aligned} \tag{9}$$

where $N \in \mathbb{N}$ is the cycle number, $C_{bat}(0)$ is the full cell capacity, and a, b are the parameters to be estimated online.

III. Online Estimation Scheme for RUL Prediction

The goal of this work is to develop an online estimation scheme that predicts battery RUL. Essentially, we estimate parameters a and b of the aging model (9) online and use the identified model to predict capacity fade. We present a novel hierarchical scheme depicted in Figure 2. The scheme consists of three stages. In Stage 1, a sliding mode observer based on the two-state thermal model is employed to simultaneously estimate unmeasured state (T_c) and unmeasured input ($\dot{Q}$), using the available online measurements of surface temperature (T_s), input current (I), and terminal voltage (V_T). Next, the estimated heat generation $\widehat{\dot{Q}}$ is passed to Stage 2, where another sliding mode observer based on the SOC-model is applied to estimate the unmeasured state (SOC) and unknown parameter (C_{bat}). Finally, Stage 3 identifies parameters of capacity fade model (9). The inputs to Stage 3 are the input current (I), estimated core temperature (T_c) and capacity (C_{bat}). In contrast to the first two stages, Stage 3 operates on a slower time scale by taking the estimated capacity value at the end of each charge-discharge cycle, and updating parameters of the aging model (9) online. For this stage, we use the nonlinear least-squares algorithm for parameter estimation. In the following subsections, we detail the design of each stage.

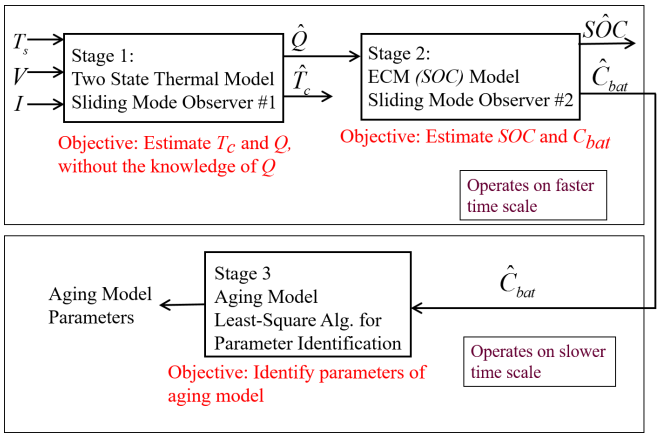

Fig. 2: Online RUL Estimation Scheme

A. Stage 1: Estimation of Core Temperature & Heat Generation

The purpose of Stage 1 is to simultaneously estimate the core temperature (unmeasured state) and heat generation (unmeasured input). We consider the following observer structure for Stage 1:

$$\dot{\widehat{T}}_c = -\frac{1}{R_cC_c}\widehat{T}_c + \frac{1}{R_cC_c}\widehat{T}_s + L_1\text{sgn}(v) \tag{10}$$

$$\dot{\widehat{T}}_s = \frac{1}{R_cC_s}\widehat{T}_c - \Big(\frac{1}{R_uC_s} + \frac{1}{R_cC_s}\Big)\widehat{T}_s + \frac{1}{R_uC_s}T_f + L_2v_1 \tag{11}$$

$$\widehat{Q} = L_1C_c\text{sgn}(v) \tag{12}$$

where L_1, $L_2 > 0$ are scalar observer gains to be designed. $\text{sgn}(\cdot)$ is the sign function. Moreover, $v_1 = \text{sgn}(T_s - \widehat{T}_s)$, and v is the filtered version of L_2v_1. In real time, v can be computed by passing L_2v_1 through a low pass filter with unity steady-state gain, i.e. $v(t) = \{\omega/(s+\omega)\}L_2v_1(t)$, where ω is the cut-off frequency. Next, we provide the convergence analysis of observer (10)-(11).

Convergence Analysis of Stage 1 Observer:

Consider the estimation error $\widetilde{T}_c = T_c - \widehat{T}_c$ and $\widetilde{T}_s = T_s - \widehat{T}_s$. Subtracting (10)-(11) from (5)-(6), the error dynamics can be written as:

$$\dot{\widetilde{T}}_c = -\frac{1}{R_cC_c}\widetilde{T}_c + \frac{1}{R_cC_c}\widetilde{T}_s + \frac{1}{C_c}\dot{Q} - L_1\text{sgn}(v) \tag{13}$$

$$\dot{\widetilde{T}}_s = \frac{1}{R_cC_s}\widetilde{T}_c - \Big(\frac{1}{R_uC_s} + \frac{1}{R_cC_s}\Big)\widetilde{T}_s - L_2\text{sgn}(\widetilde{T}_s) \tag{14}$$

We analyze error dynamics (14) by using the Lyapunov function candidate $V_1(t) = \frac{1}{2}\widetilde{T}_s^2$. The derivative of the Lyapunov function candidate V_1 is

$$\begin{aligned}\dot{V}_1 &= \widetilde{T}_s\dot{\widetilde{T}}_s \\ &= \frac{1}{R_cC_s}\widetilde{T}_c\widetilde{T}_s - \Big(\frac{1}{R_uC_s} + \frac{1}{R_cC_s}\Big)\widetilde{T}_s^2 - L_2\widetilde{T}_s\text{sgn}(\widetilde{T}_s) \\ &\le |\widetilde{T}_s|\Big(\frac{1}{R_cC_s}|\widetilde{T}_c| - L_2\Big)\end{aligned} \tag{15}$$

If the gain L_2 is chosen high enough such that

$$L_2 > \frac{1}{R_cC_s}|\widetilde{T}_c|_{\max} \tag{16}$$

then we have that $\dot{V}_1 \le 0$.

Remark 1. For the design of the observer gain L_2, we need a finite value for $|\widetilde{T}_c|_{\max}$. Essentially, $|\widetilde{T}_c|_{\max} < L_2R_cC_s$ can be viewed as a *Region of Convergence* (ROC) for the observer, which is function of the observer gain L_2. Hence, we can define an acceptable ROC for the observer and design the observer gain accordingly.

Furthermore, note from (15) that

$$\dot{V}_1 \le -\sqrt{2}\alpha\sqrt{V_1} \quad \text{where} \quad \alpha = L_2 - \frac{1}{R_cC_s}|\widetilde{T}_c|_{\max} \tag{17}$$

Applying the comparison principle on (17) yields $V_1 \le (\sqrt{V_1(0)} - \alpha t/\sqrt{2})^2$, and then the time needed for $\widetilde{T}_s$ to converge to zero is

$$t_{1f} = \frac{\sqrt{2V_1(0)}}{\alpha} \tag{18}$$

Therefore, it can be concluded that $\widetilde{T}_s \to 0$ in finite time t_{1f}, and hence, the sliding mode is attained. At the sliding mode, we have $\widetilde{T}_s = 0$ and $\dot{\widetilde{T}}_s = 0$. Substituting these expressions in (14), we can write $v = \frac{1}{R_cC_s}\widetilde{T}_c$. Next we analyze (13) using the Lyapunov function candidate $V_2(t) = \frac{1}{2}\widetilde{T}_c^2$. The derivative of Lyapunov function candidate V_2:

$$\begin{aligned}\dot{V}_2 &= \widetilde{T}_c\dot{\widetilde{T}}_c \\ &= -\frac{1}{R_cC_c}\widetilde{T}_c^2 + \frac{1}{C_c}\dot{Q}\widetilde{T}_c - L_1\widetilde{T}_c\text{sgn}\Big(\frac{1}{R_cC_s}\widetilde{T}_c\Big) \\ &\le |\widetilde{T}_c|\Big(\frac{1}{C_c}|\dot{Q}| - L_1\Big)\end{aligned} \tag{19}$$

If we choose the gain L_1 high enough such that

$$L_1 > \frac{1}{C_c}|\dot{Q}|_{\max} \tag{20}$$

we can conclude that $\dot{V}_2 \le 0$.

Remark 2. For the design of observer gain L_1, we need a finite value for $|\dot{Q}|_{\max}$. From (7), this maximum value can be determined based on *a priori knowledge* of the possible range of input current, temperature, terminal and open circuit voltages.

Similarly, the finite time for $\widetilde{T}_c$ to converge to zero is

$$t_{2f} = \frac{\sqrt{2V_2(0)}}{\beta}, \qquad \text{where} \quad \beta = L_1 - \frac{1}{C_c}|\dot{Q}|_{\max} \tag{21}$$

At the sliding mode, we have $\widetilde{T}_c = 0$ and $\dot{\widetilde{T}}_c = 0$. After $t > t_{2f} > t_{1f}$, with $\widetilde{T}_s = 0$, equation (13) simplifies to:

$$\dot{\widehat{Q}} = L_1C_c\text{sgn}(v) \tag{22}$$

B. Stage 2: Estimation of Battery SOC and Capacity

Stage 2 simultaneously estimates battery SOC (unmeasured state) and capacity (unknown parameter) by receiving heat generation estimate from Stage 1 as an input signal. We consider the following observer structure for Stage 2:

$$\dot{\widehat{SOC}} = L_3 \text{sgn}(OCV_m - \widehat{OCV}) \tag{23}$$

$$OCV_m = \frac{\hat{\dot{Q}}}{I} + V_T + \hat{T}\frac{dU}{dT} \tag{24}$$

$$\widehat{C}_{bat} = -\frac{I}{L_3 v_3} \tag{25}$$

where v_3 is the filtered version of $\text{sgn}(OCV_m - \widehat{OCV})$, computed by passing $\text{sgn}(OCV_m - \widehat{OCV})$ through a low pass filter with unity steady-state gain in real time. L_3 is the scalar observer gain to be designed. Note that $\hat{\dot{Q}}$ and $\hat{T}$ are the estimated heat generation from (22) and estimated average temperature from Stage 1. As analyzed in the previous subsection, we have $\hat{\dot{Q}} = \dot{Q}$ and $\hat{T} = T$, and hence from (7), $OCV_m = OCV$ after $t > t_{1f} > t_{2f}$. Under this scenario, we analyze the convergence of observer (23)-(24).

Remark 3. Note that (24) requires division by current $I(t)$ to reconstruct OCV_m information. Therefore, this reconstruction cannot be used under zero current scenarios. This limitation arises from the fact that the heat generation is zero under zero current (according to the model (7)). For practical implementation, this issue can be dealt with by turning off this reconstruction, and hence the output injection term of the observer, under the condition $|I(t)| < \epsilon$ where ϵ is an user-defined arbitrary small positive number.

Convergence Analysis of Stage 2 Observer:

Strict monotonicity of the OCV-SOC relationship guarantees

$$\text{sgn}(OCV - \widehat{OCV}) = \text{sgn}(SOC - \widehat{SOC}). \tag{26}$$

Remark 4. In this formulation, we have assumed that the OCV is a monotonically increasing function of SOC over the 0%-100% SOC range. Note that this assumption is already verified for most of the popular Li-ion chemistry, e.g. $LiCoO_2$ -Graphite and $LiFePO_4$-Graphite [13].

We can re-write observer (23) based on (26):

$$\dot{\widehat{SOC}} = L_3 \text{sgn}(SOC - \widehat{SOC}) \tag{27}$$

The dynamics of $\widetilde{SOC} = SOC - \widehat{SOC}$ can be written as:

$$\dot{\widetilde{SOC}} = \dot{SOC} - \dot{\widehat{SOC}} = -\frac{I}{C_{bat}} - L_3 \text{sgn}(\widetilde{SOC}) \tag{28}$$

Consider the Lyapunov function candidate $V_3(t) = \frac{1}{2}\widetilde{SOC}^2$. The derivative of V_3 along the trajectories of $\widetilde{SOC}$ is

$$\begin{aligned}\dot{V}_3(t) &= \widetilde{SOC} \cdot \dot{\widetilde{SOC}} = \widetilde{SOC}\Big(-\frac{I}{C_{bat}} - L_3 \text{sgn}(\widetilde{SOC})\Big) \\ &\leq \Big|\frac{I}{C_{bat}}\Big| |\widetilde{SOC}| - L_3 |\widetilde{SOC}| \\ &= |\widetilde{SOC}| \cdot \Big(\Big|\frac{I}{C_{bat}}\Big| - L_3\Big)\end{aligned} \tag{29}$$

Choose the gain L_3 high enough such that

$$L_3 > \frac{|I|_{\max}}{|C_{bat}|_{\min}} \tag{30}$$

Remark 5. The values for $|I|_{\max}$ and $|C_{bat}|_{\min}$ can be determined *a priori* based on knowledge of feasible input current and battery capacity range.

Similarly, the finite time for $\widetilde{SOC}$ to converge to zero is

$$t_{3f} = \frac{\sqrt{2V_3(0)}}{\gamma} \qquad \text{where} \quad \gamma = L_3 - \frac{|I|_{\max}}{|C_{bat}|_{\min}} \tag{31}$$

At the sliding mode, we have $\widetilde{SOC} = 0$ and $\dot{\widetilde{SOC}} = 0$. Substituting these expressions in (28) gives:

$$\widehat{C}_{bat} = -\frac{I}{L_3 v_3} \tag{32}$$

C. Stage 3: Online Identification of Battery Aging Model

The purpose of Stage 3 is to estimate the parameters $\theta = \begin{bmatrix} a & b \end{bmatrix}^T$ of the aging model (9) via a nonlinear least-squares identification algorithm. Define $\tilde{\theta} = \theta - \hat{\theta}$ and write (9) in terms of $\tilde{\theta} = \begin{bmatrix} \tilde{a} & \tilde{b} \end{bmatrix}^T$:

$$C_{bat}(N) = \Big[1 - (\tilde{a} + \hat{a}) \exp\Big(\frac{\tilde{b} + \hat{b}}{T_c}\Big)(Ah)^z\Big] C_{bat}(0) \tag{33}$$

Next we take the Taylor series approximation with respect to $\tilde{\theta}$ around $\tilde{\theta} = 0$

$$\begin{aligned}C_{bat}(N) \approx &\Big[1 - \hat{a} \cdot \exp\Big(\frac{\hat{b}}{T_c}\Big)(Ah)^z\Big] C_{bat}(0) \\ &- \Big[\exp\Big(\frac{\hat{b}}{T_c}\Big)(Ah)^z C_{bat}(0)\Big]\tilde{a} \\ &- \Big[\hat{a} \cdot \frac{1}{T_c} \cdot \exp\Big(\frac{\hat{b}}{T_c}\Big)(Ah)^z C_{bat}(0)\Big]\tilde{b}\end{aligned} \tag{34}$$

Re-arrange the previous expression into the matrix form

$$\begin{aligned}e_{nl} &= C_{bat}(N) - \Big[1 - \hat{a} \exp\Big(\frac{\hat{b}}{T_c}\Big)(Ah)^z\Big] C_{bat}(0) \\ &= \tilde{\theta}^T \phi\end{aligned} \tag{35}$$

where the regressor vector ϕ is defined as

$$\phi = \begin{bmatrix} -\exp\Big(\frac{\hat{b}}{T_c}\Big)(Ah)^z C_{bat}(0) \\ -\hat{a} \cdot \frac{1}{T_c} \cdot \exp\Big(\frac{\hat{b}}{T_c}\Big)(Ah)^z C_{bat}(0) \end{bmatrix} \tag{36}$$

The regressor ϕ depends upon measured signals and parameter estimates. We now choose a discrete-time least-squares parameter update law with forgetting factor and normalization

$$\hat{\theta}(N+1) = \hat{\theta}(N) + P(N)e_{nl}(N)\phi(N),\ \hat{\theta}(0) = \hat{\theta}_0 \quad (37)$$

$$P(N+1) = (1+\beta)P(N) - P(N)\frac{\phi(N)\phi^T(N)}{m^2(N)}P(N), \quad (38)$$

$$P(0) = P_0 = P_0^T \succ 0 \quad (39)$$

$$m^2(N) = 1 + \phi(N)\phi^T(N) \quad (40)$$

IV. Simulations and Discussion

In this section, we present simulation studies that demonstrate the performance of the proposed online RUL estimation scheme. The battery under consideration is a $LiFePO_4/LiC_6$ A123 26650 cell with nominal capacity 2.3 Ah. The parameter values are taken from [11]. In the plant model simulation, we incorporate the nonlinear capacity fade model (8). To illustrate the performance, we apply a repeated charge-discharge cycle to the battery model. Each cycle consists of a charging protocol [14] that charges the battery from 25% to 75% SOC, followed by a constant discharge with low C-rate that discharges the battery to 25% SOC. Figure 3 plots the evolution of current, terminal voltage, core and surface temperature in the plant, for part of one charge-discharge cycle. We repeat this cycle 200 times to test our proposed scheme. All the estimated quantities (unknown states, input and parameters) are initialized with incorrect values to illustrate the convergence properties.

A. Performance of Stage 1 and Stage 2: Core Temperature, Heat Generation, State-of-Charge and Capacity Estimation

We now consider only the first cycle. First, we evaluate the performance of observer (10)-(12) in Stage 1. The core and surface temperature estimates are initialized with incorrect values (3^oC initial error for both cases) to validate the convergence property. Figure 4 portrays the evolution of unknown state (T_c) and unknown input ($\dot{Q}$) estimation of thermal system (5)-(6). Note that with an appropriate choice of gain $L_1 = 25$ and $L_2 = 5$ as presented in (20) and (16), the convergence time for T_c and Q are $t_{1f} = 10$ sec and $t_{2f} = 12$ sec. Next, we investigate the effectiveness of state (SOC) and capacity (C_{bat}) estimation in Stage 2. Similar to the Stage 1 observer, the SOC estimate is initialized with incorrect value (15% initial error). Figure 5 shows the convergence of SOC and capacity (C_{bat}) to their true values. In this case, SOC convergence time is $t_{3f} = 60$ sec and capacity convergence time is 204 sec. These results confirm the finite-time zero error convergence analysis conclusions for the Stage 1 and 2 observers in Section III.

B. Performance of Stage 3: Parameter Identification of the Aging Model

In this section, we illustrate the performance of online aging model parameter identification. We simulate 200 cycles of the previously mentioned charge-discharge profile. The first 100 cycles are used to identify the parameters of the aging model whereas the rest are used to test the prediction performance. We initialize the parameters to incorrect values, and finally the estimated parameters $\hat{a}$ and $\hat{b}$ are obtained by algorithm (37)-(40). In the prediction phase we use these identified parameters to predict battery capacity and compare the prediction with testing data. Figure 6 illustrates the prediction performance, where the blue '+' markers represent the capacity fade prediction and the red 'o' markers represent the actual capacity fade data from the nonlinear aging model (8). The root mean square (RMS) prediction error is 0.0002 Ah compared to testing data set, meaning our proposed online estimation scheme achieves ≈0.01% error in predicting capacity fade under current usage condition, normalized against nominal cell capacity. Consequently, we simulate forward the aging model (9) with the identified parameters to predict RUL. In this case study, the predicted cycle number that reaches EOL will be 1407 cycles.

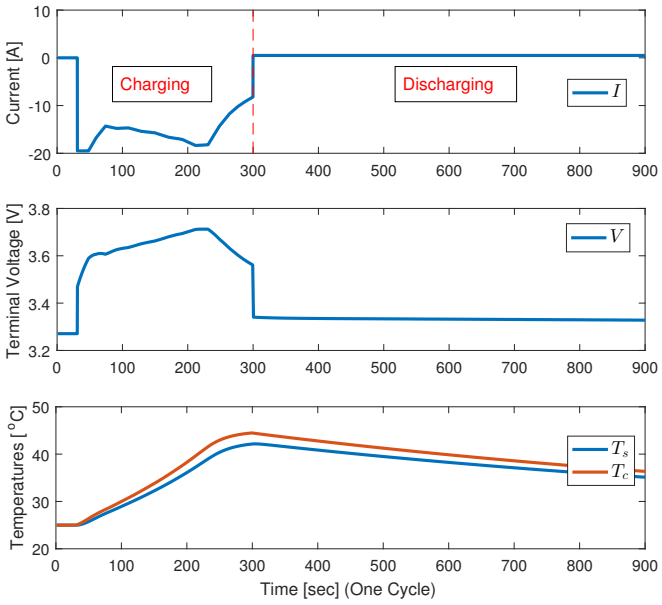

Fig. 3: Current, voltage, core temperature, and surface temperature in the plant. This charge-discharge cycle is repeated for 200 times.

V. Conclusion

This paper proposes an online Remaining Useful Life (RUL) estimation scheme for Li-ion batteries from a thermal prospective. The proposed estimation scheme consists of three stages operating in a cascaded manner. Stages 1 and 2 estimate battery core temperature, SOC and capacity based on a two-state temperature model and Coulombic SOC model utilizing sliding mode observers. The convergence for the sliding mode observers are mathematically analyzed using Lyapunov stability theory. The estimated capacity and core temperature, along with measured current, are then utilized in Stage 3 to identify a capacity fade aging model via a nonlinear least-squares algorithm. A simulation case study with 200 repeated charge-discharge cycles is presented, where the first 100 cycles are used to identify the aging model online. The

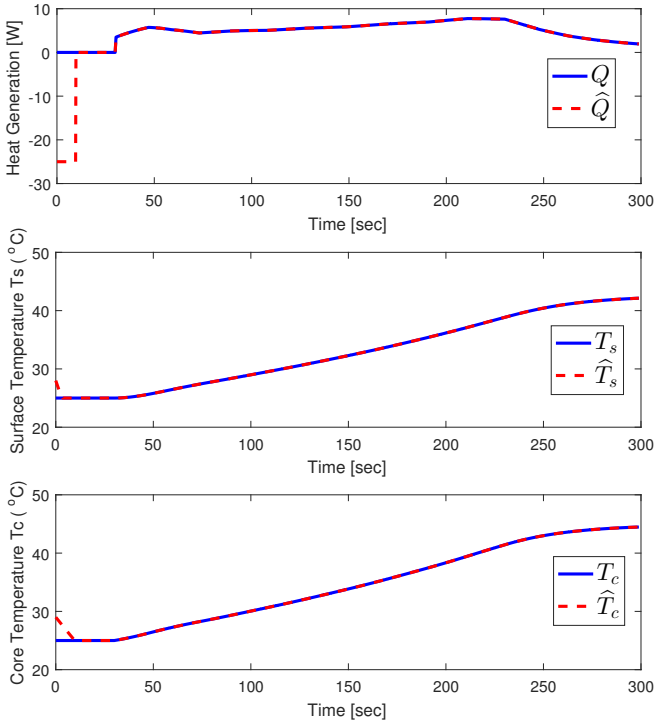

Fig. 4: Estimation performance for the first charging process, for thermal model. (a). heat generation; (b). surface temperature; (c). core temperature

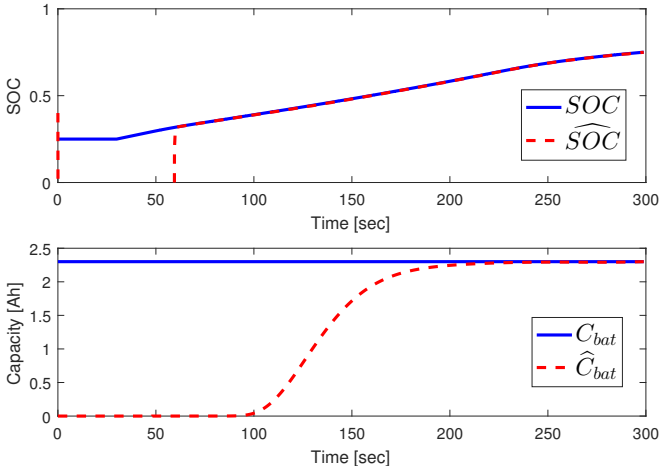

Fig. 5: Estimation performance for the first charging process, for electrical model. (a). SOC; (b). capacity (true value is 2.3 Ah)

identified aging model successfully predicts the capacity fade over the next 100 cycles. The main contribution of this paper includes online estimation of battery capacity fade from thermal perspective, by incorporating nonlinear model-based observers and least-squares algorithm. In addition, with the identified aging model, we are able to prognose the End-of-Life (EOL) of the battery. Future work will validate this estimation scheme using real battery experimental data.

REFERENCES

[1] A. Barré, B. Deguilhem, S. Grolleau, M. Gérard, F. Suard, and D. Riu, "A review on lithium-ion battery ageing mechanisms and estimations for automotive applications," *Journal of Power Sources*, vol. 241, pp. 680–689, 2013.

[2] J. Liu, A. Saxena, K. Goebel, B. Saha, and W. Wang, "An adaptive recurrent neural network for remaining useful life prediction of lithium-ion batteries," tech. rep., DTIC Document, 2010.

[3] B. Saha, K. Goebel, S. Poll, and J. Christophersen, "Prognostics methods for battery health monitoring using a bayesian framework," *IEEE Transactions on Instrumentation and Measurement*, vol. 58, no. 2, pp. 291–296, 2009.

[4] S. Tang, C. Yu, X. Wang, X. Guo, and X. Si, "Remaining useful life prediction of lithium-ion batteries based on the wiener process with measurement error," *Energies*, vol. 7, no. 2, pp. 520–547, 2014.

[5] Y. Zhou, M. Huang, Y. Chen, and Y. Tao, "A novel health indicator for on-line lithium-ion batteries remaining useful life prediction," *Journal of Power Sources*, vol. 321, pp. 1–10, 2016.

[6] M. Orchard, L. Tang, B. Saha, K. Goebel, and G. Vachtsevanos, "Risk-sensitive particle-filtering-based prognosis framework for estimation of remaining useful life in energy storage devices," *Studies in Informatics and Control*, vol. 19, no. 3, pp. 209–218, 2010.

[7] J. Wu, C. Zhang, and Z. Chen, "An online method for lithium-ion battery remaining useful life estimation using importance sampling and neural networks," *Applied Energy*, vol. 173, pp. 134–140, 2016.

[8] Y. Zhang and B. Guo, "Online capacity estimation of lithium-ion batteries based on novel feature extraction and adaptive multi-kernel relevance vector machine," *Energies*, vol. 8, no. 11, pp. 12439–12457, 2015.

[9] S. Drakunov and V. Utkin, "Sliding mode observers. tutorial," in *Decision and Control, 1995., Proceedings of the 34th IEEE Conference on*, vol. 4, pp. 3376–3378, IEEE, 1995.

[10] H. E. Perez, X. Hu, S. Dey, and S. J. Moura, "Optimal charging of li-ion batteries with coupled electro-thermal-aging dynamics," accepted in *IEEE Transactions on Vehicular Technology*, 2017.

[11] X. Lin, H. E. Perez, S. Mohan, J. B. Siegel, A. G. Stefanopoulou, Y. Ding, and M. P. Castanier, "A lumped-parameter electro-thermal model for cylindrical batteries," *Journal of Power Sources*, vol. 257, pp. 1–11, 2014.

[12] J. Wang, P. Liu, J. Hicks-Garner, E. Sherman, S. Soukiazian, M. Verbrugge, H. Tataria, J. Musser, and P. Finamore, "Cycle-life model for graphite-lifepo4 cells," *Journal of Power Sources*, vol. 196, no. 8, pp. 3942 – 3948, 2011.

[13] M. Safari and C. Delacourt, "Modeling of a commercial graphite/lifepo4 cell," *Journal of The Electrochemical Society*, vol. 158, no. 5, pp. A562–A571, 2011.

[14] H. E. Perez, S. Dey, X. Hu, and S. J. Moura, "Optimal charging of li-ion batteries via a single particle model with electrolyte and thermal dynamics," *in review*.

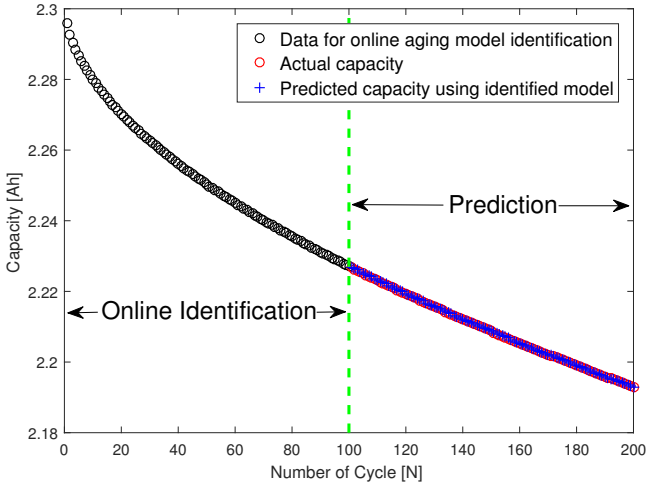

Fig. 6: Aging model parameter identification using least-squares algorithm. The first 100 data points are used for online identification, and the remaining 100 data points are for testing